

Envisioning Wheat Flour Dough as a Triphasic Medium to Predict Bubbles Stability

Arnaud Turbin-Orger, Hubert Chiron, Laurent Chaunier, Guy Della Valle*

INRA, UR 1268 Biopolymères, Interactions & Assemblages (BIA), BP 71627, 44316 Nantes, France

ABSTRACT

Recent studies of micro-X-ray tomography (XRT) at high resolution show that, at the end of fermentation, wheat flour dough can be considered a three-phase medium gas / liquid / viscoelastic matrix. Properties and distribution of each phase are determined and a capillary number is calculated in order to determine their influence on the evolution of the cellular structure.

INTRODUCTION

Wheat flour dough contains about 45% water (tot. basis) and its cellular structure is created during fermentation; during this stage, porosity increases from 0.1 to 0.7 and CO₂ bubbles are connected together, although the dough does not collapse¹. This stability could be due to the formation of a liquid foam, constituted by a liquid phase, co-continuous to the starch/gluten viscoelastic matrix^{2,3}. To determine the role of this phase in the creation of the cellular structure, the aqueous phase, so-called dough liquor (LdP), has recently been considered as a good model for these interfacial films⁴. In complement, elongational properties of dough can be determined by lubricated squeezing flow test (LSF), which underlines the importance of minor components⁵. Starting from the study of bubbles growth and coalescence in model dough systems, the aim of this study is to

determine the role of the aqueous phase and the starch/gluten matrix on the mechanisms which govern the creation of cellular structure at microscopic scale, and at macroscopic scale on the loss of stability at the end of fermentation⁶.

MATERIALS AND METHODS

Compositions of bread doughs is reported in Table 1, and procedure for preparing them described in detail elsewhere⁶. Volumic liquid fraction ϕ_{vl} is determined from concentration and density of ingredients.

N°/ing.	Water	Sugar	Fat	ϕ_{vl}	M ($\epsilon_b=1$) (kPa.s ⁿ)	n	b' (min)
1	66	0	5	0.60	12.8	0.53	23
2	60	2	2	0.58	16.9	0.42	27
3	55	15	2	0.59	14.2	0.48	25
4	65	10	10	0.63	8.6	0.60	18
5	62	0	0	0.58	17.8	0.45	24

Table 1 . Compositions of doughs for 100 g flour (Fat: rapeseed oil), and values of elongational properties and stability characteristic time.

After adapting a specific procedure to highly hydrated wheat flour doughs⁷, LSF test allowed to determine equibiaxial stress σ , Hencky strain ϵ_b , and strain rate $\dot{\epsilon}_b$, and to derive the elongational viscosity:

$$\eta = M \cdot \dot{\epsilon}_b^{n-1} \quad \text{with} \quad \epsilon_b = \text{cst} \quad (1)$$

Flow index n and consistency M are often studied to determine the impact of dough composition on cell structure creation and coalescence⁵.

Dough stability is determined by the follow-up and image analysis of dough during fermentation⁶, through the ratio R of height H to its maximum width L_{\max} , and its kinetics is adjusted by:

$$R(t) = \frac{H}{L_{\max}}(t) = a' \times \exp\left(-\frac{t}{b'}\right) + c' \quad (2)$$

With $a'+c' = 0.6$ and b' the characteristic time of stability.

Microscopic follow-up of dough during fermentation was performed by X-ray Computed Microtomography (XRT), based on the absorption contrast of materials, on ID19 ESRF line (F38-Grenoble), as detailed precedingly⁹. Analysis of 3D images allow to determine bubbles and matrix films thickness volumic distribution.

Dough liquor (LdP) is extracted according to detailed procedure⁴, and its rheological properties are determined on RFSII with imposed strain, using a cone-plane geometry. For each LdP, measurements are performed in steady and dynamic regimes. Surface tension is measured on drop Tracker (IT concept) on fresh LdP: a pending drop is formed and its surface area is continuously observed by a camera. Surface tension γ between air and LdP is determined from bubble shape using Laplace law.

RESULTS

Although rheological behavior is similar for all doughs, and marked by shear-thinning, different values of characteristic indices are obtained according to composition (Table 1). Flow index values vary in a narrow interval [0.42, 0.6], whereas consistency M varies from 8.6 kPa.sⁿ to 17.8 Pa.sⁿ, and it is inversely

correlated to ϕ_{vl} . Stability time is found to be only fairly correlated to M , suggesting that the more viscous the dough, the more stable it is; but likely other mechanisms interplay in the collapse or stability of dough during fermentation, like gas cells interactions.

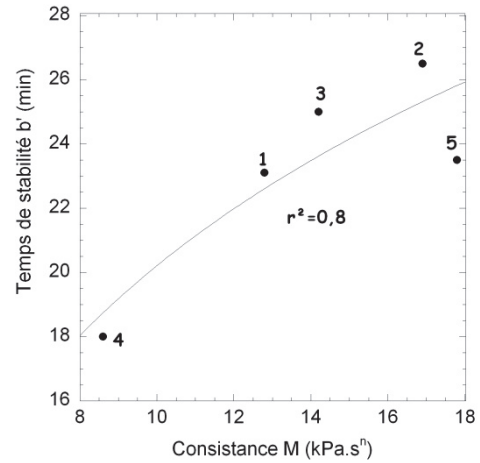


Figure 1. Variations of dough stability time with its consistency M .

In this purpose, 3D XRT images show that, for larger fermentation times, bubbles are connected to each other. For instance, for dough #4, which has a high ϕ_{vl} value, cellular structure becomes coarse and the shapes of gas cavities suggest that coalescence may have occurred.

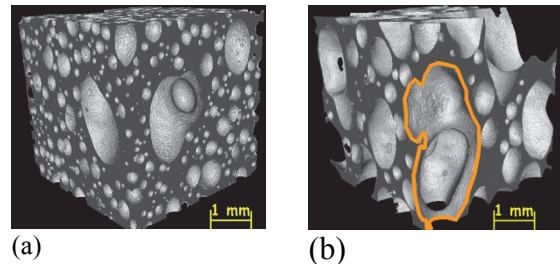


Figure 2. XRT images (ESRF) of dough#4 at $t=60$ (a) and 180 min (b) (res. 5 μ m).

Granulometry analysis allows to quantify the distributions of gas cells and cell wall sizes. When represented them for the same value of porosity ($=0.6$), they show that bubbles have a maximum size of 1 to 1.75 mm³. From these distributions, a homogeneity index of the cell structure could be defined, noted b . Conversely,

heterogeneity was mainly due to bubbles coalescence (Fig.2b). To ascertain this phenomenon, the distributions of wall thickness, obtained at P=0.6 (Fig.3) are fitted to a Normal law:

$$Y(x) = \frac{1}{\sigma * \sqrt{2 * \Pi}} * exp^{-\frac{1}{2} * (\frac{x-\mu}{\sigma})^2} \quad (3)$$

Y being the volumic fraction of walls having a thickness = x, σ being the standard deviation, and μ the mean thickness value. The curves are distinct, confirming that different cellular structures are obtained for same porosity, but all display a peak close to 0.23 mm (Fig.3).

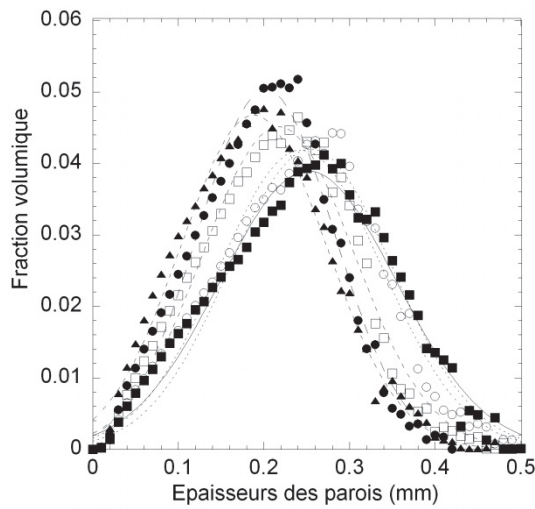


Figure 3. Cell wall thickness distributions in volumic frequency for a porosity of 0.6, and various dough ■: 1, ●: 2, ▲: 3, ○: 4, □: 5.

The volumic fraction of thinner walls (10 μ m) is not null ($\approx 2.10^{-4}$); although bubbles are connected together, they might be separated by films with a thickness lower than the XRT resolution (5 μ m). Given the size of starch granules ($\geq 5\mu$ m) and the low gluten content ($\approx 7\%$ of tot. basis), this result confirms the presence of liquid films surrounding bubbles, and avoiding their collapse^{2,3}. An order of magnitude of their thickness might be given by a critical value e_c defined by:

$$e_c = \frac{e_{min} * FreqVol}{Freq\bar{Vol}} \quad (4)$$

e_{min} being the lowest thickness detectable by XRT (10 μ m here), $FreqVol$ and $Freq\bar{Vol}$ its volumic frequency and average value, respectively, for all doughs. e_c values vary from 0.8 to 2.3 μ m, and are correlated with the homogeneity of cell structure (Fig.4).

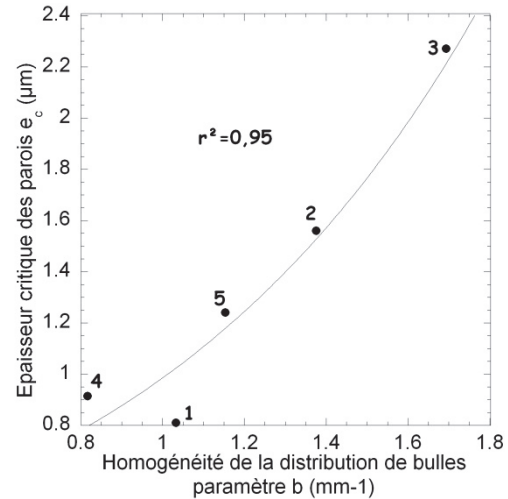


Figure 4. Variations of critical wall thickness with homogeneity of cell structure.

This correlation suggests that, when walls thickness are lower than e_c , the starch gluten matrix experiences ruptures, leading to a heterogeneous cell structure, like for dough #4, and its liquid phase becomes continuous. For thickness values larger than e_c , walls may still contain gluten and even starch. Then, the correlation of e_c with dough stability suggests that a stable dough has a homogeneous cell structure (Fig.5).

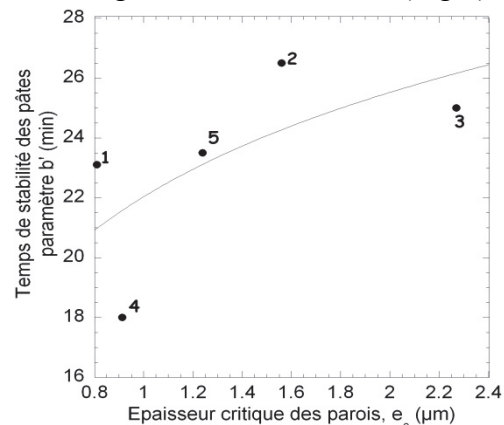


Figure 5. Variations of dough stability with critical wall thickness.

However, this correlation is not high enough, and this result suggests that the liquid phase also interplays by its rheological properties.

Every extracted dough liquor (LdP) displays an overall behavior of viscoelastic liquid with a yield stress at low strain rates, which can be fitted by a Herschel-Bulkley model:

$$\tau = \tau_0 + k \times \dot{\gamma}^n \quad (5)$$

Polysaccharides likely contribute to the viscous behavior at higher shear rate, whereas their interactions with proteins mostly influence the behavior at lower shear rate values, which results in a yield stress¹⁰. Moreover, the flow curves obtained in dynamic and steady regimes superimpose which show that Cox-Merz rule applies (Fig.6) for all dough compositions, as expected from a viscoelastic solution of polymers.

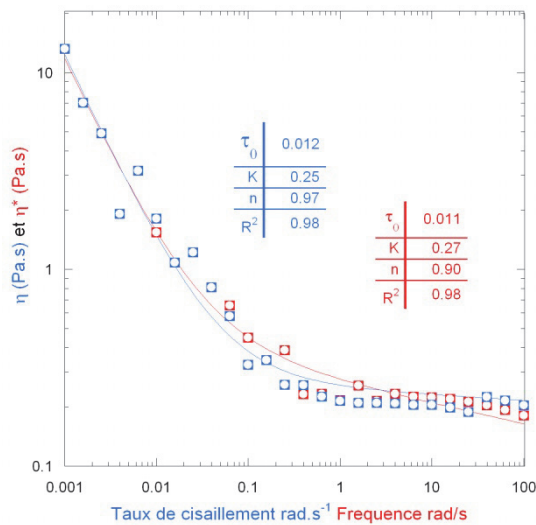


Figure 6. Variations of complex η^* and steady η shear viscosities for LdP# 4.

Then surface tension γ is found to vary from 35 to 41.2 mN/m, and it is inversely correlated to the values of yield stress. The properties of LdP are related to the dough behavior, although no direct correlation could be evidenced.

Consequently, in analogy with biphasic media¹¹, an apparent capillary Number is computed in order to integrate the influence

of the various levels of organization of dough:

$$Ca^* = (\tau_m \cdot e_c) / \gamma \quad (6)$$

Where τ_m is the elongational stress of the matrix, determined according to eq. (1) for a strain rate value of 10^{-3} s^{-1} . By computing Ca^* for all doughs, it is found that large values are found for most stable doughs and conversely, the less stable have low values of Ca^* (Fig.7).

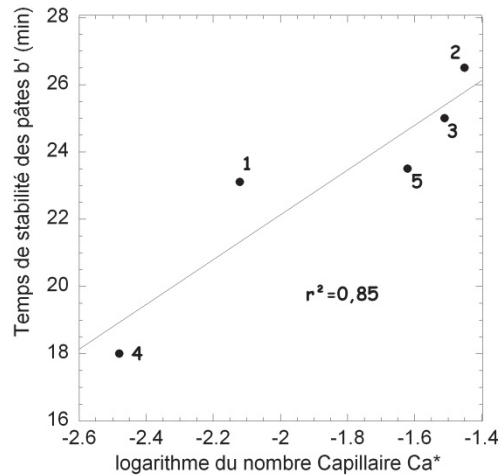


Figure 7. Variations of dough stability time with apparent capillary number.

This correlation, which should be strengthened by other experimental results, allowed to integrate various structural levels and opens practical prospects for predicting the cellular structure from the knowledge of the rheological properties of dough components.

ACKNOWLEDGMENTS

The research leading to these results has received funding from the European Community's Seventh Framework Programme (FP7/ 2007-2013) under the grant agreement FP7-222 654, Dream project: Design and development of REAListic food Models with well characterized micro- and macro structure and composition.

REFERENCES

- Babin, P., Della Valle, G., Chiron, H., Cloetens, P., Hoszowska, J., Pernot, P.,

- Réguerre, A.L., Salvo, L., Dendievel, R. (2006), "Fast X-ray tomography analysis of bubble growth and foam setting during Breadmaking", *Journal of Cereal Science*. **43**, 393-397.
2. Gan, Z., Ellis, P.R., Schofield, J.D. (1995), "Gas Cell Stabilisation and Gas Retention in Wheat Bread Dough", *Journal of Cereal Science* **21**, 215-230.
3. Mac Ritchie, F. (2005), "The liquid phase of dough and its role in baking", *Cereal Chemistry*. **82**, 20-27.
4. Salt, L.J., Wilde, P.J., Georget, D., Wellner, N., Skeggs, P.K., Mills, E.N.C. (2006), "Composition and surface properties of dough liquor", *Journal of Cereal Science*. **43**, 284-292.
5. Rouillé, J., Della Valle, G., Lefebvre, J., Sliwinski, E., Van Vliet, T. (2005), Shear and extensional properties of bread doughs affected by minor components. *Journal of Cereal Science*. **42**, 45-57.
6. Shehzad, A., Chiron, H., Della Valle, G., Kansou, K., Ndiaye, A., Réguerre, A.L. (2010). "Porosity and stability of bread dough during proofing determined by video image analysis for different compositions and mixing conditions", *Food Research International*. **43**, 1999-2005.
7. Kouassi-Koffi, J.D., Launy, B., Davidou, S., Kouamé, L.P., Michon, C. (2010). "Lubricated squeezing flow of thin slabs of wheat flour dough: comparison of results at constant plate speed and constant extension rates", *Rheol Acta* **49**, 275-283.
8. Boller, E., Tafforeau, P., Ludwig, W., Helfen, L., Weitkamp, T., Salvo, L., Baruchel, J. (2010). Techniques d'imagerie pour la caractérisation 3D des matériaux à l'ESRF. *Conférence Matériaux, Nantes*.
9. Turbin-Orger, A., Boller, E., Chaunier, L., Chiron, H., Della Valle, G., Réguerre, A.L. (2012), "Kinetics of bubbles growth in wheat flour dough during proofing studied by computed X-ray micro-tomography", *Journal of Cereal Science*, **56**, 676-683.
10. Doublier, J.L., Garnier, C., Renard, D., Sanchez, C. (2001), "Protein-polysaccharide interactions", *Current Opinion in Colloid and Interface Science*, **5**, 202-214.
11. van der Sman, R.G.M., van der Goot, A.J. (2008), "The science of food structuring", *Soft Matter*, **5**, 501-510.

